Am J Transl Res 2025;17(10):8364-8374
www.ajtr.org /ISSN:1943-8141/AJTR0164098

Original Article

Upregulation of PD-L1 and MMP9 in HR-HPV-associated cervical squamous cell carcinoma: correlation with histological progression and immune microenvironment remodeling

Ying Ruan[1], Runyu Xia[2], Shuai Luo[1], Ran Li[1], Xiaoli Dong[1], Jinjing Wang[1], Hong Zheng[1]

[1]Department of Pathology, Affiliated Hospital of Zunyi Medical University, Zunyi 563000, Guizhou, China; [2]Zunyi Medical University, Zunyi 563000, Guizhou, China

Received February 22, 2025; Accepted October 11, 2025; Epub October 25, 2025; Published October 30, 2025

Abstract: Objective: To investigate the expression and significance of programmed death-ligand 1 (PD-L1), matrix metalloproteinase 9 (MMP9), and tissue inhibitor of metalloproteinases 3 (TIMP3) in HR-HPV-associated cervical squamous cell carcinoma (CSCC) and precancerous lesions. Methods: A retrospective analysis of 180 cervical cancer and lesion cases were performed, dividing them into a HR-HPV infection group (n=120) and a non-infection group (n=60). Immunohistochemical staining was used to assess the expression of PD-L1, MMP9, and TIMP3 proteins in both groups. Results: PD-L1 and MMP9 expression was significantly higher in HR-HPV-infected specimens compared to non-infected ones across all lesion grades (P<0.05). Both markers exhibited progressive upregulation correlating with increasing lesion severity from inflammation to low-grade squamous intraepithelial lesion (LSIL), high-grade squamous intraepithelial lesion (HSIL), and CSCC. Quantitative analysis showed significantly higher integrated optical density values of PD-L1 and MMP9 in HR-HPV-positive HSIL and CSCC compared to HR-HPV-negative cases (P<0.05). In carcinoma patients, PD-L1 expression was correlated with HR-HPV infection status and histological grade (P<0.05), while TIMP3 showed an inverse correlation with MMP9 (r=-0.348, P=0.028). ROC analysis demonstrated superior diagnostic performance for PD-L1 (AUC=0.863) and MMP9 (AUC=0.731) compared to TIMP3 (AUC=0.175) in distinguishing CSCC from non-malignant lesions. Conclusion: The expression rates of PD-L1 and MMP9 increased progressively with lesion severity from inflammation through LSIL, HSIL, to CSCC. Additionally, higher-grade cervical squamous cell carcinoma exhibited stronger PD-L1 positivity in HR-HPV-infected cases.

Keywords: Programmed death-ligand 1 (PD-L1), matrix metalloproteinase 9 (MMP9), tissue inhibitor of metalloproteinases 3 (TIMP3), high-risk human papillomavirus (HR-HPV), cervical squamous cell carcinoma (CSCC)

Introduction

Cervical cancer remains the fourth most common malignancy among women globally, posing a significant public health burden [1]. Persistent infection with high-risk human papillomavirus (HR-HPV) is well-established as a critical etiological factor driving the progression of cervical precancerous lesions to invasive squamous cell carcinoma with HR-HPV DNA detected in approximately 96% of cervical cancer cases [1]. Emerging evidence highlights the oncogenic roles of HPV-encoded E6/E7 proteins, which not only promote genomic instability but also enhance immune evasion by upregulating the programmed death-1/programmed death-ligand 1 (PD-1/PD-L1) axis. Notably, therapeutic strategies targeting PD-1/PD-L1 immune checkpoints have demonstrated promising clinical efficacy in metastatic cervical cancer, emphasizing the translational relevance of this pathway [2].

Beyond viral oncogenesis, dynamic remodeling of the extracellular matrix (ECM) within the tumor microenvironment critically influences cancer progression and therapeutic resistance. The ECM serves as a structural and biochemical scaffold regulating cellular adhesion, signaling, and homeostasis. Pathological alterations in the ECM, characterized by aberrant degradation or deposition, are involved in processes

https://doi.org/10.62347/BYVL1679

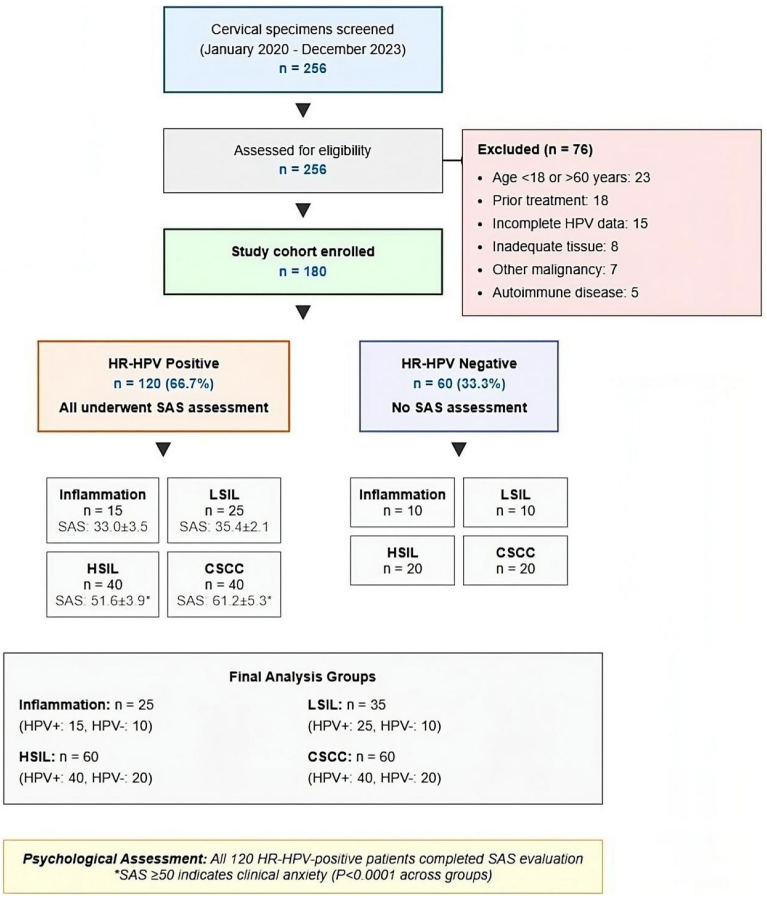

Figure 1. Flow diagram showing the selection and allocation of study participants. From an initial screening of 256 cervical specimens, 76 were excluded based on predefined criteria. The final cohort of 180 eligible patients was stratified by HPV status and histopathological diagnosis into four groups. HR-HPV: High-risk human papillomavirus; LSIL: Low-grade squamous intraepithelial lesion; HSIL: High-grade squamous intraepithelial lesion; CSCC: Cervical squamous cell carcinoma; SAS: Self-rating Anxiety Scale.

ranging from tumor invasion to metastatic niche formation [3]. Matrix metalloproteinases (MMPs), particularly MMP-9, play a central role in ECM remodeling by cleaving key substrates, including collagens, elastin, fibronectin, and laminin. While elevated MMP-9 expression has paradoxically been associated with favorable outcomes in cervical cancer, its context-dependent roles warrant further investigation [3].

Counterbalancing MMP activity, tissue inhibitor of metalloproteinases-3 (TIMP3) functions as a multifunctional regulator with both MMP-dependent and -independent antitumor effects. Although TIMP3 downregulation through epigenetic silencing (e.g., promoter hypermethylation) or miRNA-mediated repression is frequently observed in malignancies, conflicting reports suggest elevated TIMP3 levels in advanced cancers, indicating its complex dual roles in tumor-stroma crosstalk [4, 5]. Despite these advances, the interplay between HR-HPV infection and the expression profiles of PD-L1, MMP-9, and TIMP3 in cervical carcinogenesis remains underexplored. Therefore, this study aims to systematically evaluate the clinical and prognostic significance of PD-L1, MMP-9, and TIMP3 expression across the histopathological spectrum of HR-HPV-associated cervical squamous cell carcinoma (CSCC) and its precursor lesions.

Materials and methods

Case selection

This retrospective study analyzed 180 cervical specimens diagnosed at Zunyi Medical University's Affiliated Hospital between January 2020 and December 2023. The cases were stratified into four histopathological groups: chronic inflammation (n=25), low-grade squamous intraepithelial lesion (LSIL, n=35), high-grade squamous intraepithelial lesion (HSIL, n=60), and CSCC (n=60). These were further divided by HR-HPV status into 120 HPV-positive and 60 HPV-negative cases (**Figure 1**). As this was a retrospective analysis using archived tissue samples and clinical data collected during routine clinical care, we obtained a waiver of informed consent from the Ethics Committee of Zunyi Medical University (Approval No: KLL-2021-355).

Eligibility criteria: Women aged 18-60 years with histopathologically confirmed cervical lesions (chronic cervicitis, LSIL/CIN1, HSIL/CIN2-3, or CSCC) were included. All patients were treatment-naïve, had adequate tissue samples (>100 evaluable cells), and complete HPV testing results. Exclusion criteria included autoimmune diseases, immunodeficiency, active non-

HPV infections, hepatic dysfunction (alanine aminotransferase/aspartate aminotransferase [ALT/AST] >3×ULN), renal impairment (estimated glomerular filtration rate [eGFR] <30 mL/min/1.73 m^2), severe anemia (hemoglobin <8 g/dL), thrombocytopenia (platelets <50×10^9/L), leukopenia (white blood cells <3×10^9/L), concurrent malignancies, pregnancy/lactation, or incomplete pathological data.

Histopathological classification: Specimens were classified according to the WHO 2020 criteria: (1) Chronic inflammation: Non-dysplastic cervicitis; (2) LSIL: CIN1/mild dysplasia; (3) HSIL: CIN2-3/moderate to severe dysplasia; (4) CSCC: Invasive squamous cell carcinoma with >1 mm stromal invasion.

CSCC subclassification: The 60 CSCC cases were further categorized by: (1) Histological grade: Grade I (well-differentiated, n=12, 20%); Grade II (moderately differentiated, n=40, 66.7%); Grade III (poorly differentiated, n=8, 13.3%). (2) FIGO staging (2018): Stage I (n=56, 93.3%); Stage II (n=2, 3.3%); Stage III (n=2, 3.3%). (3) HPV status: CSCC-HR-HPV positive (n=40, 66.7%); CSCC-HR-HPV negative (n=20, 33.3%).

Data collection

Comprehensive baseline data were retrospectively extracted from electronic medical records and pathological archives, including: (1) demographic characteristics (age at diagnosis, stratified by decade); (2) clinical parameters, including histopathological classification (per WHO/Bethesda criteria) and FIGO staging (for carcinoma cases); (3) virological status determined via PCR with Hybribio assays or hybrid capture methodology (HR-HPV positive/negative); (4) laboratory indices covering hemoglobin levels (g/dL), platelet counts (×10^3/μL), and hepatic/renal function markers (ALT, AST, eGFR).

Psychological assessment

All HR-HPV-positive patients completed the Self-rating Anxiety Scale (SAS) at diagnosis before any treatment intervention. The SAS, a validated 20-item questionnaire, assesses anxiety symptoms with scores ranging from 20-80: <50 indicates normal, 50-59 mild anxiety, 60-69 moderate anxiety, and ≥70 severe anxiety. Questionnaires were administered by trained nurses in a private setting. Patients with incomplete responses were excluded from psychological analysis. This assessment aimed to evaluate the psychological burden across the spectrum of cervical pathology.

Immunohistochemical staining

Immunohistochemical staining was used to assess PD-L1, MMP9, and TIMP3 protein expression across the groups. Specimens were fixed in neutral buffered formalin (10%), followed by standard dehydration, paraffin embedding, and sectioning at a thickness of 3 μm. Staining was performed using the MaxVision two-step method. Primary antibodies included polyclonal antibodies for TIMP3 (dilution ratio 1:200) and ready-to-use monoclonal antibodies for PD-L1 and MMP9, all procured from Shanghai Gene Company. Phosphate-buffered saline (PBS) was used as a negative control in place of primary antibodies. The staining results were independently evaluated by two pathologists using a double-blind method.

In immunohistochemical staining, PD-L1 positivity was localized to the cell membrane, while TIMP3 and MMP9 staining was cytoplasmic. PD-L1 expression was quantified using the combined positive score (CPS) method: CPS = (number of PD-L1-positive tumor cells, lymphocytes, and macrophages)/(total number of viable tumor cells) × 100%. A CPS of ≥1% was considered PD-L1 positive [2]. For TIMP3, MMP9, and PD-L1, the scoring combined staining intensity and the percentage of positive cells. Intensity scoring: 0 for no staining, 1 for yellow, 2 for brown, 3 for dark brown. Percentage scoring: 0 for ≤5%, 1 for 6%-25%, 2 for 26%-50%, 3 for 51%-75%, and 4 for >75%. The final score, calculated by multiplying intensity and percentage scores, classified expression levels: >4 indicated high expression, ≤4 indicated low expression, and no staining indicated negativity. For quantitative analysis, five different stained areas per slide were examined, and the integrated optical density (IOD) values were determined using Image-Pro Plus 6.0.

Quantitative image analysis

Protein expression was quantified using integrated optical density (IOD) measurements with Image-Pro Plus 6.0 software (Media Cybernetics). Five non-overlapping high-power fields (400×) were randomly captured and analyzed, with background correction against negative controls. Color deconvolution separated

Table 1. Demographic characteristics and psychological assessment of study cohorts stratified by HPV status and lesion type

Groups	Number of cases	HR-HPV+/-	Age (years, mean ± SD) HR-HPV+	Age (years, mean ± SD) HR-HPV-	Self-rating anxiety scale (SAS) score HR-HPV+
Inflammatory group	25	15/10	40.87±11.78*	46.10±14.75	23.542±6.681***
LSIL group	35	25/10	35.56±9.179**	42.80±15.06	30.833±3.227***
HSIL group	60	40/20	38.55±11.91**	39.90±11.09*	52.500±1.768*
CSCC group	60	40/20	57.55±11.73	55.25±10.37	60.00±2.394
Total number of cases	180	120/60	120	60	120
χ^2/F		0.8571	29.79	5.662	295.0
P-value		0.8358	0.0001	0.0059	<0.0001

Note: Compared with CSCC group, *P<0.05, **P<0.01, ***P<0.001. HR-HPV: High-Risk Human Papillomavirus; SAS: Self-rating Anxiety Scale; LSIL: Low-Grade Squamous Intraepithelial Lesion; HSIL: High-Grade Squamous Intraepithelial Lesion; CSCC: Cervical Squamous Cell Carcinoma.

the DAB chromogen from hematoxylin counterstaining, and IOD values were calculated as the product of optical density and positive area, normalized to total area. The mean IOD across five fields represented the final expression intensity for each sample. Reproducibility was excellent, with intra-observer and inter-observer intraclass correlation coefficients of 0.92 and 0.89, respectively. Quality control involved blinded re-analysis of 10% of slides, achieving >95% concordance.

Statistical methods

Data analysis was conducted using SPSS 19.0 software. Measurement data are expressed as mean ± standard deviation (±SD). Comparisons across multiple groups were performed using one-way analysis of variance (ANOVA), followed by Tukey's post-hoc test. For two-group comparisons, the independent sample t-test was used. Count data were expressed as rates and evaluated using the chi-square test and Fisher's exact test as appropriate. Spearman's rank correlation coefficient was used to assess the association between protein expressions. Diagnostic efficacy of the proteins was evaluated using receiver operating characteristic (ROC) curve analysis. The significance level was set at α=0.05, with P<0.05 considered statistically significant.

Results

Comparison of patient characteristics and baseline demographics

Patient demographics, including age and SAS scores, are presented in **Table 1**. In the CSCC group, the mean age of HR-HPV-positive patients was 57.55±11.73 years, while the mean age of HR-HPV-negative patients was 55.25± 10.37 years. Although the means were close, the variance in age across all lesion groups in the HR-HPV-positive group was significant (F=29.79, P<0.001). Further intergroup comparisons revealed that the age of patients in the CSCC group was significantly higher than in the inflammation group, LSIL group, and HSIL group (all P<0.05). Notably, the age of HR-HPV-negative patients in the HSIL group was significantly lower than in the CSCC group (P<0.05), suggesting a potential link between age, lesion progression, and viral clearance ability. Psychological assessment using the SAS was conducted in all 120 HR-HPV-positive patients. Anxiety levels showed significant progression with lesion severity (F=295.0, P<0.0001). Patients with HSIL and CSCC exceeded the clinical threshold for anxiety (≥50 points), with CSCC patients showing moderate anxiety levels.

Comparison of expression patterns of TIMP3, MMP9, and PD-L1 across lesion grades

Table 2 presents the positive expression rates of TIMP3, MMP9, and PD-L1 proteins, stratified by lesion type and HR-HPV status. Overall expression patterns showed significant differences across lesion grades for all three markers (P<0.001). PD-L1 expression was absent in the inflammatory and LSIL groups but emerged in the HSIL group (25% in HR-HPV+, 35% in HR-HPV-) and increased markedly in the CSCC group (85% in HR-HPV+, 90% in HR-HPV-). MMP9 expression showed progressive upregulation

Table 2. Positive expression of TIMP3, MMP9, and PD-L1 proteins in HR-HPV infected and non-infected groups [number of cases (%)]

Groups	Number of cases	Infected group Number of positive cases (%)	Number of cases	Non-infected group	X^2	*p*-value
TIMP3						
Inflammatory group	15	10 (66.67)	10	8 (80.00)	0.529	0.467
LISL group	25	23 (92.00)	10	7 (70.00)	2.823	0.093
HSIL group	40	33 (82.5)	20	18 (90.00)	0.588	0.443
CSCC group	40	7 (17.5)	20	7 (35.00)	2.283	0.131
X^2		49.812		14.775		
p-value		<0.001		0.021		
MMP9						
Inflammatory group	15	3 (20.00)		1 (10.00)	0.446	0.504
LISL group	25	4 (16.00)		2 (20.00)	0.080	0.777
HSIL group	40	34 (85.00)		15 (75.00)	0.891	0.345
CSCC group	40	39 (97.5)		20 (100)	0.508	0.476
X^2		55.127		33.086		
p-value		<0.001		<0.001		
PD-L1						
Inflammatory group		0 (0)		0 (0)		
LISL group		0 (0)		0 (0)	-	-
HSIL group		10 (25.00)		7 (35.00)	0.657	0.418
CSCC group		34 (85.00)		18 (90.00)	0.288	0.591
X^2		65.742		33.874		
p-value		65.742		<0.001		

Note: TIMP3: Tissue Inhibitor of Metalloproteinase 3; MMP9: Matrix Metalloproteinase 9; PD-L1: Programmed Death-Ligand 1; HR-HPV: High-Risk Human Papillomavirus; LSIL: Low-Grade Squamous Intraepithelial Lesion; HSIL: High-Grade Squamous Intraepithelial Lesion; CSCC: Cervical Squamous Cell Carcinoma.

from inflammatory lesions through CSCC. In contrast, TIMP3 expression was highest in LSIL and HSIL but decreased significantly in CSCC (P<0.05). Notably, within each lesion category, the expression rates of TIMP3, MMP9, and PD-L1 did not differ significantly between HR-HPV-positive and HR-HPV-negative cases (P>0.05), suggesting that while HPV status influences expression intensity (as shown by IOD values in **Table 3**), it does not affect the proportion of positive cases within each histological grade.

Comparison of IOD values of TIMP3, MMP9, and PD-L1 proteins in HR-HPV infected and non-infected groups

In HSIL specimens, MMP9 IOD values were 1.8-fold higher in HR-HPV-positive cases compared to HR-HPV-negative cases (P=0.002). Similarly, PD-L1 expression was 2.3-fold higher in HR-HPV-positive HSIL cases versus negative cases (P=0.009). In CSCC, this pattern persisted, with MMP9 showing 2.0-fold (P=0.002) and PD-L1 showing 1.5-fold (P=0.039) higher expression in HR-HPV-positive specimens. TIMP3 expression showed no significant differences between the infection groups (P>0.05, **Table 3**).

Association between HR-HPV infection rate and expression levels of TIMP3, MMP9, PD-L1 in the carcinoma group and pathological parameters

In the carcinoma group, typical immunohistochemistry staining images for TIMP3, MMP9, and PD-L1 expressions are illustrated in **Figure 2**. The relationship between HR-HPV infection and the expression levels of TIMP3, MMP9, and PD-L1 with pathological parameters is shown in **Table 4**. Both HR-HPV infection and PD-L1 expression were significantly associated with histological grade (P=0.005 and P=0.012, respectively). All Grade III tumors were HR-HPV-

Table 3. IOD values of TIMP3, MMP9, and PD-L1 proteins in HR-HPV infected and non-infected groups [($\bar{x}$±SD)]

Groups	Number of cases (n=120)	Infected group		Number of cases (n=60)	Non-infected group		*t*	*p*-value
		Number of positive cases	IOD value		Number of positive cases	IOD value		
TIMP3								
Inflammatory group	15	10	54.59±22.05	10	8	141.1±102.0	2.179	0.066
LISL group	25	23	64.74±76.74	10	7	75.39±20.85	0.3241	0.757
HSIL group	40	33	88.46±38.83	20	18	67.40±44.67	1.402	0.179
CSCC group	40	7	33.92±16.95	20	7	45.82±27.27	1.153	0.293
F			3.263			4.370		
P value			0.071			0.057		
MMP9								
Inflammatory group	15	3	31.38±0.000		1	33.77±0.000	-	-
LISL group	25	4	42.85±24.37		2	40.47±13.25	0.08975	0.943
HSIL group	40	34	115.8±52.72		15	65.15±36.24	3.720	0.002
CSCC group	40	39	155.8±83.86		20	76.25±32.40	3.691	0.002
F			6.121			-		
P value			0.011			-		
PD-L1								
Inflammatory group	15	0	0		0	0	0	0
LISL group	25	0	0		0	0	0	
HSIL group	40	10	63.03±18.44		7	27.51±13.23	3.769	0.009
CSCC group	40	34	118.5±62.44		18	78.72±27.82	2.235	0.039
t			2.655			6.473		
P value			0.026			<0.001		

Note: IOD: Integrated Optical Density; TIMP3: Tissue Inhibitor of Metalloproteinase 3; MMP9: Matrix Metalloproteinase 9; PD-L1: Programmed Death-Ligand 1; HR-HPV: High-Risk Human Papillomavirus; LSIL: Low-Grade Squamous Intraepithelial Lesion; HSIL: High-Grade Squamous Intraepithelial Lesion; CSCC: Cervical Squamous Cell Carcinoma.

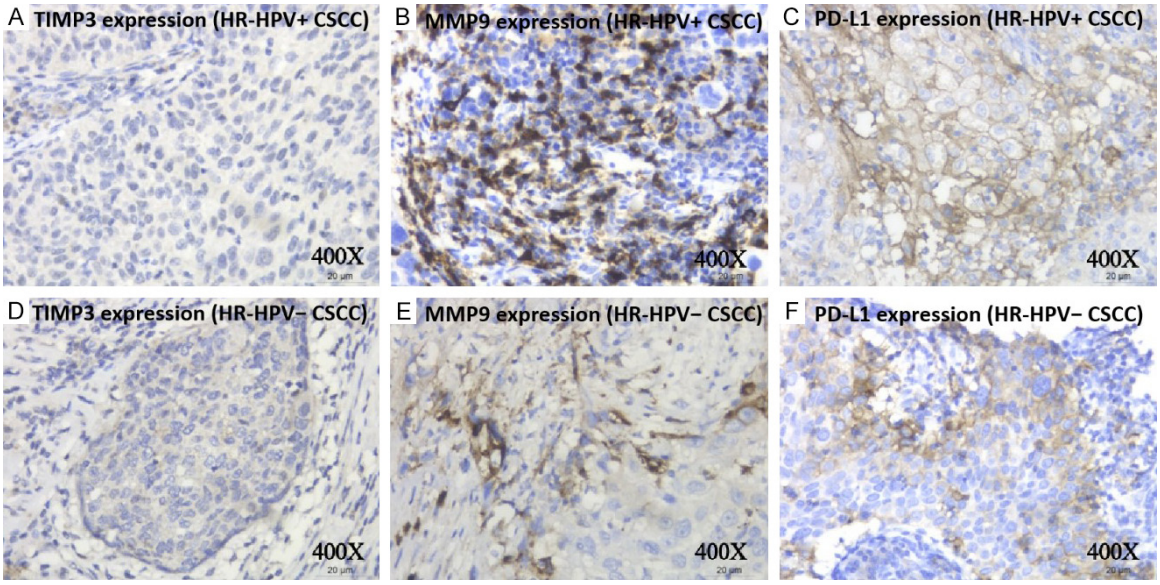

Figure 2. Immunohistochemistry staining of the expression of TIMP3, MMP9, and PD-L1 proteins in the carcinoma group. A-C. Images respectively show the expression of TIMP3, MMP9, and PD-L1 proteins in the HR-HPV infected CSCC group; 400X; D-F. Images respectively show the expression of TIMP3, MMP9, and PD-L1 proteins in the non-infected CSCC group; Images captured at 400× magnification (scale bar: 20 μm). TIMP3: Tissue Inhibitor of Metalloproteinase 3; MMP9: Matrix Metalloproteinase 9; PD-L1: Programmed Death-Ligand 1; HR-HPV: High-Risk Human Papillomavirus; CSCC: Cervical Squamous Cell Carcinoma.

Table 4. Relationship between HR-HPV infection and expression levels of TIMP3, MMP9, PD-L1 with pathological parameters in the CSCC cohort [n (%)]

Parameter	Type	Number of cases	HR-HPV infection rate	TIMP3 positivity rate	MMP9 positivity rate	PD-L1 positivity rate
Age	<50 years old	15	11 (73.33)	1 (6.67)	14 (93.33)	15 (100.00)
	≥50 years old	45	29 (64.44)	13 (28.89)	45 (100.00)	37 (82.22)
	χ^2		0.400	1.988	-	-
	P-value		0.527	0.159	0.250	0.188
Stage	Stage I	56	36 (64.28)	13 (23.21)	55 (98.21)	49 (87.50)
	Stage II	2	2 (100.00)	0	2 (100.00)	2 (100.00)
	Stage III	2	2 (100.00)	1 (50.00)	2 (100.00)	1 (50.00)
	χ^2		-	-	-	-
	P-value		0.342	0.782	0.801	0.264
Histologic grade	Grade I	12	10 (83.33)	9 (75.00)	11 (91.67)	7 (58.33)
	Grade II	40	22 (55.00)	5 (12.5)	40 (100.00)	38 (95.00)
	Grade III	8	8 (100.00)	0	8 (100.00)	7 (87.50)
	χ^2		10.517	-	-	8.911
	P-value		0.005	0	0.333	0.012
Vascular invasion	+	2	0	1 (50.00)	2 (100.00)	2 (100.00)
	-	58	40 (68.96)	13 (22.41)	57 (98.27)	50 (86.21)
	χ^2		-		-	-
	P-value		0.107	0.415	1.000	1.000

HR-HPV: High-Risk Human Papillomavirus; TIMP3: Tissue Inhibitor of Metalloproteinase 3; MMP9: Matrix Metalloproteinase 9; PD-L1: Programmed Death-Ligand 1; Grade I/II/III: Histological differentiation grade; Stage I/II/III: FIGO clinical stage.

positive (100%), compared to 83% of Grade I and 55% of Grade II tumors. PD-L1 positivity was highest in Grade II tumors (95%) and lowest in Grade I tumors (58%). Neither TIMP3 nor MMP9 expression correlated significantly with clinicopathological parameters, although MMP9 expression was nearly universal (>91%) across all grades.

Analysis of the relationship between the expression of TIMP3, MMP9, and PD-L1 proteins in patients with cervical lesions at different stages in HR-HPV infected and non-infected groups

Spearman correlation analysis in CSCC patients revealed a significant inverse correlation between TIMP3 and MMP9 expression (r=-0.348, P=0.028) in the HR-HPV-infected group (**Figure 3A**). No significant correlations were observed between PD-L1 and either TIMP3 (r=0.142, P=0.382) or MMP9 (r=0.089, P=0.584). In HR-HPV-negative cases, all pairwise correlations were non-significant (P>0.05). Additionally, no significant correlations were detected between TIMP3, MMP9, and PD-L1 under other pathological conditions (P>0.05).

Diagnostic value of TIMP3, MMP9, and PD-L1 protein detection in CSCC

In the HR-HPV-infected group, ROC curve analysis was conducted to assess the diagnostic value of TIMP3, MMP9, and PD-L1 expression in CSCC. The area under the curve (AUC) values were 0.175 for TIMP3, 0.731 for MMP9, and 0.863 for PD-L1 (**Figure 3B**). In the non-infected group, the AUCs were 0.262 for TIMP3, 0.775 for MMP9, and 0.862 for PD-L1 (**Figure 3C**). These results indicate that the diagnostic value of PD-L1 and MMP9 expression in CSCC is superior to that of TIMP3 in both groups. Furthermore, combined diagnostic curve analysis revealed that the combination of TIMP3, MMP9, and PD-L1 demonstrated good diagnostic capability, with an AUC of 0.810, indicating robust performance in discriminating disease status (**Figure 3D**). Detailed information is listed in **Table 5**.

Discussion

MMP9, a 92-kDa zinc-dependent endopeptidase, is the largest molecular weight member of the MMP family. It is primarily secreted as a

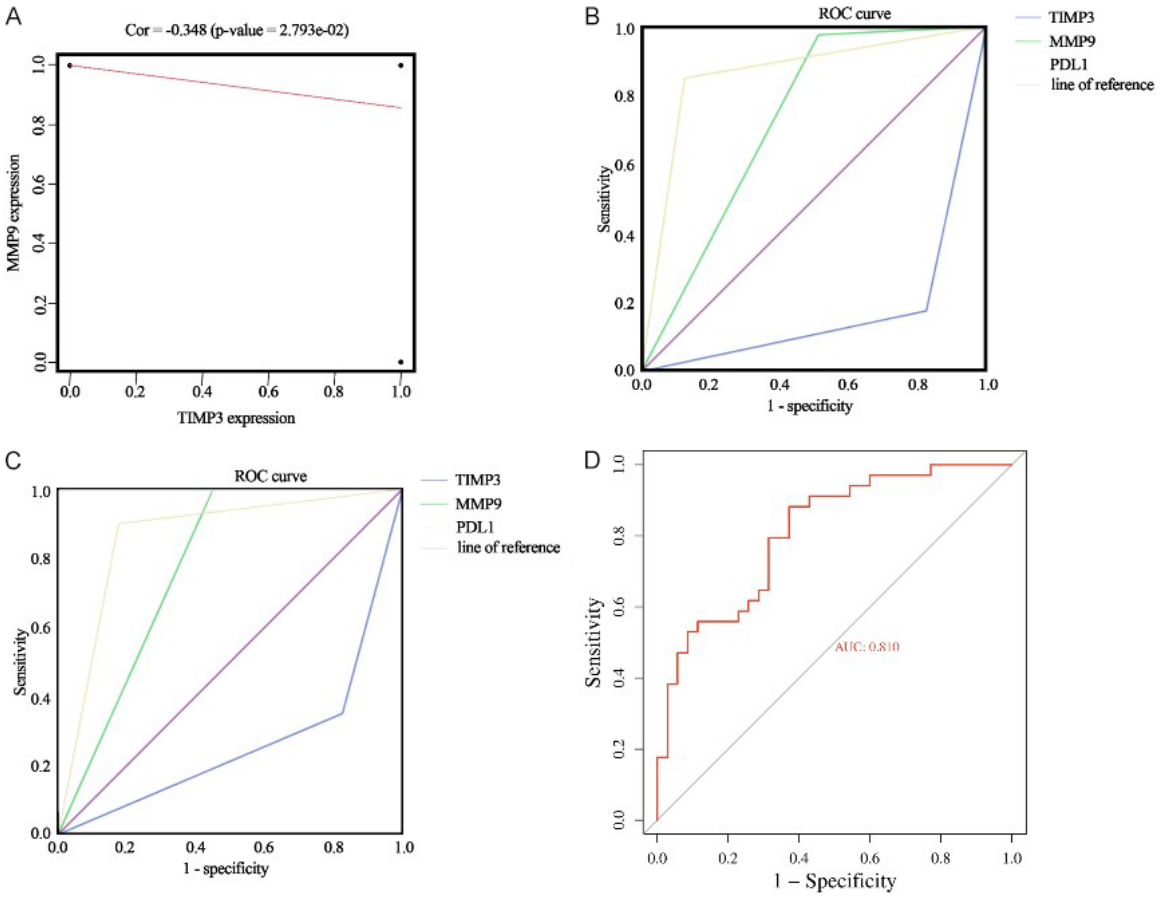

Figure 3. Composite diagnostic performance analysis. A. Spearman correlation analysis for TIMP3 and MMP9 in the HR-HPV infected group. B. Area under the ROC curve for TIMP3, MMP9, and PD-L1 in the HR-HPV infected group. C. Area under the ROC curve for TIMP3, MMP9, and PD-L1 in the non-infected group. D. Area under the ROC curve for the combination of TIMP3, MMP9, and PD-L1. ROC: Receiver Operating Characteristic; AUC: Area Under the Curve; TIMP3: Tissue Inhibitor of Metalloproteinase 3; MMP9: Matrix Metalloproteinase 9; PD-L1: Programmed Death-Ligand 1.

zymogen by various cellular components, including vascular endothelial cells, tumor-associated macrophages, malignant epithelial cells, and polymorphonuclear leukocytes [3, 5-7]. Proteolytic activation of MMP9 converts this latent pro-enzyme into functional type IV collagenase (EC 3.4.24.35), which promotes neovascularization through basement membrane degradation and facilitates tumor cell extravasation via ECM remodeling. Our immunohistochemical analysis revealed a progressive upregulation of MMP9 correlating with histopathological severity, with markedly higher expression in HR-HPV-positive specimens. This HPV-mediated dysregulation may create an immunosuppressive microenvironment conducive to neoplastic progression, aligning with recent studies demonstrating MMP9-dependent recruitment of myeloid-derived suppressor cells in HPV-associated malignancies. Specifically, the HR-HPV-positive cohort exhibited 1.8-fold higher MMP9 IOD values compared to HPV-negative specimens, suggesting that HR-HPV infection may potentiate MMP9-mediated stromal remodeling via either direct viral oncoprotein activity (E6/E7-induced transcriptional activation) or indirect modulation of tumor microenvironmental factors. This dysregulation further contributes to the creation of an immunosuppressive tumor microenvironment, as evidenced by MMP9's role in recruiting myeloid-derived suppressor cells in HPV-related malignancies. Therefore, HR-HPV infection significantly upregulates MMP9 expression, fostering a tumor-promoting microenvironment conducive to neoplastic progression.

As a member of the tissue inhibitor of metalloproteinases (TIMP) family, TIMP3 is a critical

Table 5. Diagnostic performance metrics for TIMP3, MMP9, and PD-L1 in differentiating CSCC from non-cancerous lesions

Biomarker	Group	AUC (95% CI)	Optimal Cutoff*	Sensitivity (%)	Specificity (%)	Youden Index	PPV (%)	NPV (%)
TIMP3	HR-HPV+	0.175 (0.091-0.259)	<30 IOD	17.5	17.5	-0.65	9.6	29.8
	HR-HPV-	0.262 (0.120-0.405)	<35 IOD	35.0	50.0	-0.15	31.8	52.6
MMP9	HR-HPV+	0.731 (0.643-0.819)	>95 IOD	97.5	48.8	0.463	48.8	97.5
	HR-HPV-	0.775 (0.661-0.889)	>85 IOD	100.0	55.0	0.550	57.1	100.0
PD-L1	HR-HPV+	0.863 (0.786-0.939)	>80 IOD	85.0	87.5	0.725	77.3	92.1
	HR-HPV-	0.862 (0.759-0.966)	>75 IOD	90.0	82.5	0.725	75.0	93.3
Combined	All cases	0.810 (0.745-0.875)	-	88.3	73.3	0.616	62.3	92.5

*Optimal cutoff values are based on IOD (Integrated Optical Density) measurements PPV: Positive Predictive Value; NPV: Negative Predictive Value. Note: TIMP3 shows inverse diagnostic performance (AUC<0.5) as its expression decreases in CSCC, making low values diagnostic for cancer rather than high values.

regulator of MMP9 activity, exhibiting potent inhibitory effects against MMP9, a key metalloproteinase involved in ECM degradation [8-10]. The dynamic equilibrium between TIMPs and MMPs is vital for tumor invasion and metastasis. Disruption of this balance, particularly a relative decrease in TIMP levels compared to MMPs, leads to reduced inhibition of MMP activity. This results in enhanced ECM degradation, facilitating tumor cell penetration through the basement membrane and increasing the likelihood of hematogenous or lymphatic metastasis. Our research found an increase in both the positive expression rate and the IOD value of TIMP3 in precancerous lesions. However, these levels decreased in CSCC. Notably, in HR-HPV-infected CSCC cases, TIMP3 IOD values significantly decreased, indicating that reduced TIMP3 expression correlates with tumor advancement and poorer prognosis. Interestingly, an increase in TIMP3 expression in HR-HPV-infected HSIL was observed, suggesting its potential role in tumor progression and its utility as an early marker for cancer transformation. However, the diagnostic value of TIMP3 in CSCC was relatively low, warranting further investigation and validation in larger cohorts.

The PD-L1 protein, as the ligand for PD-1, plays a crucial role in immune system suppression. It transmits inhibitory signals that induce T cells into a resting state, suppressing the proliferation of CD8+ T cells in lymph nodes and impeding their ability to recognize cancer cells. This mechanism not only decreases T cell proliferation but may also trigger apoptosis [11]. These actions facilitate immune evasion by cancer cells, significantly contributing to tumor development. This study established that PD-L1 expression was exclusive to the HSIL and CSCC groups, with a statistically significant variance in IOD values ($P<0.05$). Furthermore, the HR-HPV-infected group exhibited higher PD-L1 expression compared to the non-infected group, consistent with findings by Allouch et al. [12-14]. PD-L1 levels were significantly elevated in HPV-related CIN and CC tissues compared to non-infected patients and normal cervical tissues, highlighting HPV infection as a critical factor in cervical lesion progression. This phenomenon is attributed to the interaction between HPV infection and cellular processes: after HPV infection, the E6 protein encoded by the virus binds to the tumor suppressor gene product P53, leading to abnormal expression of P53. This aberration stimulates overexpression of TGF-β1, which triggers an inflammatory response [15]. To counteract inflammation, the body enhances the PD-1/PD-L1 interaction, leading to lymphocyte apoptosis and immune system activation. This process inhibits lymphocyte proliferation and suppresses Th1 release from CD4+ cells, thereby mitigating the inflammatory response. Moreover, this study suggests that HPV binding to the PD-L1 locus may enhance the amplification of the PD-L1 allele's 3'-untranslated region (3'-UTR), leading to elevated PD-L1 expression. This amplification potentially activates the PD-1/PD-L1 signaling pathway, negatively regulating the immune response in HPV-related CSCC, thereby influencing the progression of HPV-associated CIN. These findings provide theoretical support for utilizing PD-L1-targeted immunotherapy in HPV-infected patients. Additionally, our study reveals a correlation between PD-L1 expres-

sion in cancer groups, HR-HPV infection status, and key pathological parameters, including histological grading, suggesting that HR-HPV infection may contribute to accelerated tumor progression.

In both HR-HPV-infected and non-infected groups, ROC curve analysis was employed to evaluate the diagnostic value of TIMP3, MMP9, and PD-L1 in CSCC. PD-L1 and MMP9 expression levels were found to be more indicative than TIMP3, highlighting their strong association with cervical tumor development. These findings position PD-L1 and MMP9 as promising therapeutic targets and biomarkers for CSCC progression. Spearman's correlation analysis revealed no significant association between TIMP3 expression and either MMP9 or PD-L1. The lack of correlation could be attributed to the limited sample size of the study. In contrast, a positive correlation was observed between MMP9 and PD-L1 expression, suggesting that the co-expression of MMP9 and PD-L1 is associated with the development of CIN and cervical tumors.

This study has several limitations. First, the cross-sectional design precludes establishing causality between HR-HPV infection and biomarker expression changes during cervical carcinogenesis. Second, the single-center cohort may not fully represent all populations, particularly given regional differences in HPV genotype prevalence. The retrospective nature of the study also means that confounders such as smoking and contraceptive use were not controlled. Technical limitations include the semi-quantitative nature of immunohistochemistry and potential variability between PD-L1 antibody clones. Additionally, TIMP3/MMP9 expression was assessed at a single time point, missing potential dynamic changes during disease progression. Lastly, while the overall sample size was adequate, subgroup analyses, particularly for Grade III tumors, were underpowered. Therefore, a prospective multi-center study is needed to validate these biomarkers across diverse populations.

Conclusion

This study demonstrates that PD-L1 and MMP9 expression levels escalate in tandem with the severity of cervical lesions, with these proteins exhibiting a positive correlation in their expression. Furthermore, HR-HPV infection is associated with heightened expression of these markers. A decrease in TIMP3 expression may also be linked to tumor progression. In carcinoma cases, a significant relationship was found between PD-L1 expression, HR-HPV infection status, and key pathological parameters, including histological grading.

Acknowledgements

This research was funded by the Scientific research project of Guizhou Provincial Health Commission (grant number gzwkj2022-192).

Disclosure of conflict of interest

None.

Address correspondence to: Hong Zheng, Department of Pathology, Affiliated Hospital of Zunyi Medical University, Zunyi 563000, Guizhou, China. Tel: +86-0851-28608743; E-mail: hongzhengdr@163.com

References

[1] Stolnicu S, Allison D, Patrichi A, Flynn J, Iasonos A and Soslow RA. Invasive squamous cell carcinoma of the cervix: a review of morphological appearances encountered in human papillomavirus-associated and papillomavirus-independent tumors and precursor lesions. Adv Anat Pathol 2024; 31: 1-14.

[2] Lukovic J, Pintilie M, Han K, Fyles AW, Bruce JP, Quevedo R, Pugh TJ, Fjeldbo CS, Lyng H and Milosevic MF. An immune gene expression risk score for distant metastases after radiotherapy for cervical cancer. Clin Cancer Res 2024; 30: 1200-1207.

[3] Padežnik T, Oleksy A, Cokan A, Takač I and Sobočan M. Changes in the extracellular matrix in endometrial and cervical cancer: a systematic review. Int J Mol Sci 2023; 24: 5463.

[4] Lee WT, Wu PY, Cheng YM and Huang YF. Tissue inhibitor of metalloproteinase 3: unravelling its biological function and significance in oncology. Int J Mol Sci 2024; 25: 3191.

[5] Yang D, Fan L, Song Z, Fang S, Huang M and Chen P. The KMT1A/TIMP3/PI3K/AKT circuit regulates tumor growth in cervical cancer. Reprod Biol 2022; 22: 100644.

[6] Yang XZ, Cui SZ, Zeng LS, Cheng TT, Li XX, Chi J, Wang R, Zheng XF and Wang HY. Overexpression of Rab1B and MMP9 predicts poor survival and good response to chemotherapy in patients with colorectal cancer. Aging (Albany NY) 2017; 9: 914-931.

[7] Lorenc Z, Waniczek D, Lorenc-Podgórska K, Krawczyk W, Domagała M, Majewski M and

Mazurek U. Profile of expression of genes encoding matrix metallopeptidase 9 (MMP9), matrix metallopeptidase 28 (MMP28) and TIMP metallopeptidase inhibitor 1 (TIMP1) in colorectal cancer: assessment of the role in diagnosis and prognostication. Med Sci Monit 2017; 23: 1305-1311.

[8] Liu W, Li M, Chen X, Zhang D, Wei L, Zhang Z, Wang S, Meng L, Zhu S and Li B. MicroRNA-373 promotes migration and invasion in human esophageal squamous cell carcinoma by inhibiting TIMP3 expression. Am J Cancer Res 2016; 6: 1-14.

[9] Coates-Park S, Lazaroff C, Gurung S, Rich J, Colladay A, O'Neill M, Butler GS, Overall CM, Stetler-Stevenson WG and Peeney D. Tissue inhibitors of metalloproteinases are proteolytic targets of matrix metalloproteinase 9. Matrix Biol 2023; 123: 59-70.

[10] Bi X, Lou P, Song Y, Sheng X, Liu R, Deng M, Yang X, Li G, Yuan S, Zhang H, Jiao B, Zhang B, Xue L, Liu Z, Plikus MV, Ren F, Gao S, Zhao L and Yu Z. Msi1 promotes breast cancer metastasis by regulating invadopodia-mediated extracellular matrix degradation via the Timp3-Mmp9 pathway. Oncogene 2021; 40: 4832-4845.

[11] Fu H, Fu Z, Mao M, Si L, Bai J, Wang Q and Guo R. Prevalence and prognostic role of PD-L1 in patients with gynecological cancers: a systematic review and meta-analysis. Crit Rev Oncol Hematol 2023; 189: 104084.

[12] Allouch S, Malki A, Allouch A, Gupta I, Vranic S and Al Moustafa AE. High-risk HPV oncoproteins and PD-1/PD-L1 interplay in human cervical cancer: recent evidence and future directions. Front Oncol 2020; 10: 914.

[13] Santoro A, Angelico G, Inzani F, Arciuolo D, d'Amati A, Addante F, Travaglino A, Scaglione G, D'Alessandris N, Valente M, Tinnirello G, Raffone A, Narducci N, Cianfrini F, Bragantini E and Zannoni GF. The emerging and challenging role of PD-L1 in patients with gynecological cancers: an updating review with clinico-pathological considerations. Gynecol Oncol 2024; 184: 57-66.

[14] Aghbash PS, Hemmat N, Baradaran B, Mokhtarzadeh A, Poortahmasebi V, Oskuee MA and Baghi HB. The effect of Wnt/β-catenin signaling on PD-1/PDL-1 axis in HPV-related cervical cancer. Oncol Res 2022; 30: 99-116.

[15] Birrer MJ, Fujiwara K, Oaknin A, Randall L, Ojalvo LS, Valencia C and Ray-Coquard I. The changing landscape of systemic treatment for cervical cancer: rationale for inhibition of the TGF-β and PD-L1 pathways. Front Oncol 2022; 12: 814169.